International Research Journal of Engineering and Technology (IRJET) e-ISSN: 2395-0056
Volume: 09 Issue: 02 | April 2022 www.irjet.net p-ISSN: 2395-0072

Prediction of Vapor-Liquid Equilibrium of Ternary System (Benzene + Cyclohexane + Anisole) using Multilayer Perceptron Neural Network based models

Vishakha A Lakshete[1], Veena Patil-Shinde[2*]

[1]Postgrauduate Student (M.Tech), Chemical Engineering Department, Bharati Vidyapeeth (Deemed to be University), College of Engineeering, Pune -India
[2]Associate Professor, Chemical Engineering Department, Bharati Vidyapeeth (Deemed to be University), College of Engineeering, Pune -India

---

Abstract - *In the chemical industry, vapor-liquid equilibrium (VLE) data are essential for the design, analysis, control, and modeling of process equipment such as distillation columns, absorbers, and reactors. The usually employed feed-forward neural network, the multi-layer perceptron (MLP), was used to develop MLPNN-based models for VLE prediction in this study. The MLPNN approximates nonlinear relationships that exist between the variables in an input data set and the output data set associated with it. Experimental data was used to develop MLPNN-based VLE models for predicting the vapor phase composition of a ternary system (benzene + cyclohexane + anisole). A physical property of pure components (acentric factor) and thermodynamic parameters (equilibrium temperature, liquid phase composition) are included as the input space for the model development. An error-back propagation (EBP) approach is used to train the proposed MLPNN-based model. The experimental data was split at random, with 75% of the data used as the training set for constructing the models and 25% of the data used as the test set for evaluating the models generalization ability. The predicted values are in good agreement with the corresponding experimental values, indicating that the proposed models have good prediction accuracy and generalization ability.*

Key Words: Vapor-liquid equilibrium; Artificial neural network; Data prediction; Thermodynamic models.

1. INTRODUCTION

Vapor-liquid equilibrium data are necessary for the design, analysis, control, and development of various chemical processes [1, 2]. Phase equilibrium and in particular vapor-liquid equilibrium (VLE) is an important factor for the designing and modeling of separation processes like distillation, extraction, absorption and adsorption [3]. VLE is a condition where a liquid and its vapor state are in equilibrium with each other. In other words, a state where the rate of evaporation of liquid mixture equals the rate of condensation of vapor mixture on a molecular level [4]. Accurate measurements of VLE through experimentation for ternary or higher order systems are time-consuming, tedious, and expensive. It is not always feasible to conduct VLE experiments at all ranges of pressures and temperatures practically. Consequently, conventional thermodynamic models are used for the estimation of vapor-liquid equilibrium.

Although, conventional thermodynamic models such as the *equation of state* (EoS) and *activity-coefficient* models are used to estimate VLE data, these models necessitate a thorough understanding of the physicochemical phenomena that underlie the process [5]. Thermodynamic models used to predict VLE becomes trickier for system of non-ideal components because it involves determination of the number of thermodynamic parameters such as various *adjustable parameters*, binary *interaction parameter* (BIP), etc. Estimation of these parameters in order to get the best set by iterative methods is often tedious and time consuming exercise [6].

Second (i.e. *empirical*) approach for VLE modeling is data-driven for which detailed knowledge of physico-chemical phenomena is not required. These models use linear or nonlinear regression methods in developing the models. Although, linear regression method is applicable for the systems containing linear VLE behavior (ideal systems), most of the real systems exhibit nonlinear VLE behavior which depends on operating parameters. Thus, selection of an accurate data-fitting function (nonlinear) is difficult. Subsequently, to overcome above mentioned difficulties for conventional thermodynamic models and use of regression methods for VLE modeling, there is need to explore alternative nonlinear modeling technique.

As an alternative to conventional thermodynamic models and regression-based modeling, an artificial intelligence (AI) based nonlinear modeling formalism, particularly artificial neural networks (ANNs) [7] is employed. In the study of thermodynamics, this approach is often used to predict vapor-liquid equilibrium [8]. Besides, several researchers have been used artificial neural networks (ANN) for modeling of realistic phenomena in various scientific fields. The ANN technique has been used, for instance, in the prediction of high pressure VLE of binary systems [9], prediction of CO_2 mole fraction in liquid and vapor phase for binary system

[10], predictions of bubble point pressure and vapor phase composition of binary systems [11], prediction of VLE data for binary and ternary systems using radial basis function network [12], Prediction of VLE data for binary systems containing propane [13], explored artificial neural networks for the modeling of intermolecular and interatomic potential energy surfaces [14], prediction of °API gravity of crude oils [15], prediction of gasification performance parameters by using AI-based formalisms [16,17].

In the present study, feed-forward artificial neural network namely, multi-layer perceptron (MLP) has been utilized to develop the models to predict mole fraction of benzene (y_1) and cyclohexane (y_2) in vapor phase for ternary system (*benzene* + *cyclohexane* + *anisole*). An exhaustive literature search indicates that, this is first instance where in MLPNN-based models are developed for VLE prediction for the avowed ternary system. Experimental VLE data reported in literature [18] is used to develop the proposed MLPNN-based models, the input space and outputs to be predicted are specified in Table 1. The predicted values were compared with its corresponding experimental values which give good prediction accuracy and generalization ability for the developed model.

The structure of this paper is as follows. In Section 2, titled "Conventional thermodynamic models," different thermodynamic models exploited for VLE predictions are briefly explained. The next Section, "Artificial intelligence (AI) based modeling techniques" presents an overview of artificial neural networks and multi-layer perceptron. The data utilized in the MLPNN-based modeling of vapor phase composition are detailed in Section 4. The section, named "Results and Discussion," discusses the MLPNN-based models for predicting the mole fraction of benzene (y_1) and cyclohexane (y_2) in vapor phase. The study's principal findings are reported in the "Conclusion" section.

Table-1: Inputs and outputs of the two MLPNN-based models developed in this study

Model	No. of inputs	Model Inputs	Model outputs
I	6	Temperature (T); mole fractions of benzene (x_1), and cyclohexane (x_2) in liquid phase; acentric factors of benzene (ω_1), cyclohexane (ω_2) and anisole (ω_3)	Mole fraction of benzene in the vapor phase (y_1)
II	6	Temperature (T); mole fractions of benzene (x_1), and cyclohexane (x_2) in liquid phase; acentric factors of benzene (ω_1), cyclohexane (ω_2) and anisole (ω_3)	Mole fraction of cyclohexane in the vapor phase (y_2)

2. CONVENTIONAL THERMODYNAMIC MODELS

2.1 Equation of State Models

Vapor-liquid equilibrium data are usually estimated using thermodynamic models which are based on the criterion of phase equilibrium i.e. the chemical potentials of each of the components in each of the phases are equal. A conventional method used to predict the VLE is the *equation of state* (EoS). It is a competent tool for calculating phase equilibrium and thermodynamic properties of systems in pure or mixture form. *Equation of state* (EoS) are widely used in various practical and theoretical studies such as the petroleum industry, chemical process design, reservoir fluids, etc., further these can be applied to systems containing hydrocarbons, but it is difficult for systems that contain polar compounds. Since it is the first equation used to predict vapor-liquid coexistence, Van der Waals equation is the basis for prediction of VLE by equation of states [19]. Next, Redlich-Kwong equation of state [20] improved the Van der Waals equation by adjusting Van der Waals attractive pressure term that improves the prediction of vapor phase physical properties. Soave proposed significant changes to the Redlich-Kwong equation in order to improve the accuracy of phase behavior predictions in the critical zone [21], For tackling both liquid and vapor properties near-equilibrium conditions, the Peng-Robinson equation of state was proposed [22]. This equation is good for improving the accuracy of the prediction of liquid densities [23]. Since design, operation, control, and modeling of various chemical processes are based on the thermodynamic models and VLE predictions, it is most essential that they are easy to use and needs less number of inputs, and able to give accurate predictions.

2.2 Activity Coefficient Models

There are various methods available for the prediction of VLE such as, analytical solution of groups method (ASOG) [24], universal functional-group activity coefficients (UNIFAC) method, Van Laar, two constant margules, universal quasi-chemical (UNIQUAC) equation, non-random two-liquid (NRTL), Wilson [25]. All of the previous mentioned thermodynamic VLE models are applied for moderately non-ideal systems. For non-polar solvents such as hydrocarbons, alcohols, ketones UNIQUAC, Wilson and NRTL models gives good predictions. UNIFAC method is used in the design calculations of distillation columns [26].

3. ARTIFICIAL INTELLIGENCE (AI) BASED MODELING TECHNIQUES

Artificial Intelligence (AI) is a branch of computer science, intended for the development of computers to employ in human like thought processes such as learning, reasoning, and self-correction. AI is basically concerned

with the development of techniques and algorithms, which allow computers to "learn" and utilize this knowledge to solve problems such as function approximation and classification. Machine learning (ML) based modeling formalisms, such as support vector regression (SVR) [27], and AI-based modeling formalisms, such as artificial neural networks (ANNs) and genetic programming (GP) [28], are commonly employed as alternatives to regression-based modeling. They found various applications in the field of thermodynamics. A widely used AI-based modeling technique named artificial neural network is described briefly in the next section.

3.1 Artificial Neural Networks (ANNs)

Artificial neural networks originate from the study of methods for information processing in the biological nervous system, especially the human brain. They are based on the concept that obscure nonlinear interrelationships exist between dependent and independent variables can be learned by highly interconnected networks of simple processing units (artificial nodes). Learning takes place in the human brain in a network of neurons connected by dendrites, axons, and synapse. Dendrites are signal receiving connections of a neuron and the axon is its transmitting connection. The junctions where axon branches are connected to dendrites of numerous other neurons is called as synapses. An artificial neural network may be classified according to direction of information flow in it. Three types of connectivity patterns exists i.e. feed-forward, feed-back and recurrent. Once the model is trained with ANN architecture, then the developed model is ready to predict the outputs for new input data set, which is not utilized to train the model.29 ANN has specific applications such as data processing, pattern recognition, and the nonlinear control through the learning process.30 Feed-forward neural network (FFNN) architecture namely, multi-layer perceptron (MLP) and radial basis function network (RBFN) are most widely used to build a model.

3.2 Multi-layer Perceptron Neural Network

A multi-layer perceptron neural network (MLPNN) has a feed-forward structure i.e. flow of information is only in forward (one) direction, it approximates nonlinear relationships existing between variables of an input and the associated output data set [31]. The MLPNN architecture with one hidden layer is depicted in Fig. 1. Its structure normally consists of three layers: an input layer, a middle layer known as the hidden layer, and an output layer, each with N, M, and S processing units. Each layer contains a number of neurons (nodes). The number of neurons (n) in the input layer equals the number the inputs given to the MLP neural network, and the number of neurons (s) in the output layer equals the number of outputs in the MLP neural network. The number of hidden layers and the number of nodes in the hidden layer are adjustable parameters, and these are chosen heuristically on the basis of good output prediction accuracy and generalization ability of the model. Each node is linked to all nodes in the next layer through connection weights i.e. between input and hidden layers and between hidden and output layers. An MLP neural network also has a bias node in hidden and input layers which has a fixed output of +1.

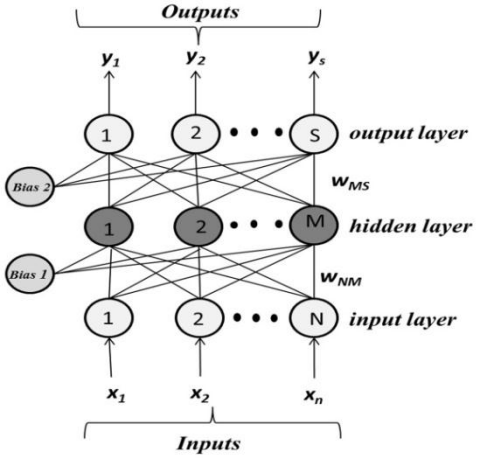

Fig-1: Schematic of one hidden layer multiple input-multiple output (MIMO) MLP Network

A single hidden layer MLP neural network is shown in the Fig.1, each input node in the input layer passes the information to each hidden node in the hidden layer and the hidden nodes pass the net activation through the appropriate nonlinear transfer function (also called as squashing function) to compute their outputs [28]. When input vector x_p is applied to the input-layer, each hidden layer neuron first computes the activation according to the weighted-sum of its inputs using the following equation.

$$net_{pm}^{h} = (\mathbf{w}_m^h)^T \mathbf{x}_p + \theta_m^h = \sum_{i=1}^{n} w_{mi}^h x_{pi} + \theta_m^h$$

$$= w_{m1}^h x_{p1} + w_{m2}^h x_{p2} + \cdots + w_{mn}^h x_{pn} + \theta_m^h; \quad m = 1, \ldots \ldots, M \tag{1}$$

where, net_{pm}^h represent activation of m^{th} hidden layer neuron. The vector $\mathbf{w}_m^h$ denotes the weights of the connections linking the input layer nodes to the m^{th} hidden node, and θ_m^h represents the strength of the link between the bias and m^{th} hidden node. The output of m^{th} hidden unit, $\hat{y}_{pm}^h$ when p^{th} input vector is applied to the network, is evaluated using a nonlinear transfer function. The outputs of the processing nodes in first hidden layer form inputs to the nodes in the subsequent layer; this layer could be another hidden layer, or an output layer. The outputs of these nodes are computed similarly as shown in Eq (2). It may, however, be noted that output

layer neurons can use either linear or a nonlinear transfer function to compute their outputs. The output layer units, indexed as s (=1,2,…,S) determine their activation as the weighted-sum of the hidden layer outputs $\hat{\boldsymbol{y}}_{pj}^{h}$ (j =0,1,2,…,m) as,

$$net_{ps}^{o} = (\mathbf{w}_{s}^{o})^{\mathrm{T}}\,\hat{\boldsymbol{y}}_{p}^{h} + \theta_{s}^{o} = \sum_{j=0}^{m} w_{sj}^{o}\,\hat{\boldsymbol{y}}_{pj}^{h}$$

$$= w_{s0}^{o}\,\hat{\boldsymbol{y}}_{p0}^{h} + w_{s1}^{o}\,\hat{\boldsymbol{y}}_{p1}^{h} + \cdots + w_{sm}^{o}\,\hat{\boldsymbol{y}}_{pm}^{h} + \theta_{s}^{o};\quad s = 1, \ldots\ldots, S \tag{2}$$

Different types of transfer functions have been used, such as linear, step threshold, ramp threshold, logistic sigmoid, hyperbolic tangent, and Gaussian [29]. In the present study, logistic sigmoid and pure linear transfer functions are used to compute the output of the hidden and output layer, respectively and are represented as below:

Logistic sigmoid function,

$$f(x) = \frac{1}{1 + e^{-x}} \tag{3}$$

Linear function,

$$f(x) = ax \tag{4}$$

The training of an MLP neural network is accomplished by using the error-back propagation (EBP) algorithm [32], which is based on a nonlinear version of the Windrow-Hoff rule known as the generalized delta rule (GDR). The error-back propagation algorithm is a supervised method of learning with two phases: propagation and weight update. The input variables are given and transmitted through the network to calculate the output values during the first phase. The value of some preset error-function is computed by comparing calculated output values to the correct answer. The error is then fed back through the network using various mechanisms. The method modifies weight of each connection in the second phase to reduce the error functions value by a small amount. The training has been continued until the networks performance is satisfactory. The trained network will next be verified using the test data set, which was not included in the training process. The root mean squared error (RMSE) is a commonly used error function that is calculated as follows,

$$RMSE = \sqrt{\frac{\sum_{i=1}^{N_{dp}} (y_{i,exp} - y_{i,pre})^2}{N_{dp}}} \tag{5}$$

Where N_{dp} denotes the number of data patterns in the example set; i is the pattern index; $y_{i,exp}$ is the i^{th} experimental value; $y_{i,pre}$ is the corresponding MLPNN-predicted output. The detailed method to obtain an optimal MLP neural network model can be found in various researches [30, 31].

4. DATA

In the present study, to develop MLPNN-based VLE models, experimental VLE data has been collected from the literature.18 Source and ranges of experimental conditions such as temperature, pressure, liquid and vapor phase composition are given in Table 2. The Z-transformation method is used to normalize the experimental data utilized for this modeling study. The experimental data set was split at random, with 75% of the data used as the training set for constructing MLPNN-based models and 25% of the data used as the test set for evaluating the generalization ability of the constructed models. The normalized variables were obtained by following method:

$$\hat{x}_{n}^{j} = \frac{x_{n}^{j} - \bar{x}_{n}}{\sigma_{n}};\quad \mathrm{j} = 1, 2, \ldots, N_{dp} \tag{6}$$

Where, N_{dp} represents the number of data patterns in the experimental data set; $\hat{x}_{n}^{j}$ (n=1, 2,..., N; N=6) denotes the normal score (standardized variable) pertaining to the values of six inputs listed in Table 1. x_{n}^{j} represents the j^{th} value of n^{th} un-normalized input variable, x_{n}; $\bar{x}_{n}$ represents the mean of x_{n}, and σ_{n} refers to the standard deviation of x_{n}. Similar to the model inputs, the outputs were normalized as follows:

$$\hat{y}_{q}^{j} = \frac{y_{q}^{j} - \bar{y}_{q}}{\sigma_{y_q}};\quad \mathrm{j} = 1, 2, \ldots, N_{dp} \tag{7}$$

Where, $\hat{y}_{q}^{j}$ (q=1,..., Q; Q=2) denotes the normal score (standardized variable) pertaining to the values of two outputs listed in Table1. y_{q}^{j} represents the j^{th} value of q^{th} un-normalized output variable, y_{q}; $\bar{y}_{q}$ refers mean of y_{q}, and σ_{y_q} refers standard deviation of y_{q}. The inputs for MLPNN-based model-I and II are same but outputs are different. The mean and standard deviation values used in the Eqs.(6) and (7) are given in Table 3, where $\bar{x}_1$, $\bar{x}_2$, $\bar{x}_3$, $\bar{x}_4$, $\bar{x}_5$, $\bar{x}_6$ and σ_1, σ_2, σ_3, σ_4, σ_5, σ_6 respectively, represents the mean and standard deviation values of temperature (T), mole fraction of benzene (x_1) and cyclohexane (x_2) in liquid phase, and acentric factors of benzene (ω_1), cyclohexane (ω_2), and anisole (ω_3).

Table-2: Source and ranges of experimental data used for the development of MLPNN-based model I and II

System	Temperature (T) (K)	Pressure (P) (kPa)	Mole fraction of benzene in liquid phase (x_1)	Mole fraction of cyclohexane in liquid phase (x_2)	Mole fraction of benzene in vapor phase (y_1)	Mole fraction of cyclohexane in vapor phase (y_2)	N_{dp}
Benzene (1) Cyclohexane (2) Anisole (3)	351.03-421.09	101.32	0.019-0.980	0.008-0.959	0.023-0.990	0.010-0.974	117

N_{dp} is the number of data patterns

Table-3: Mean and standard deviation magnitudes in respect to inputs and outputs of two MLPNN based models

Model	Model Inputs		Model Outputs	
	Mean	Standard deviation	Mean	Standard deviation
I	$\bar{x}_1 = 354.12$ (K); $\bar{x}_2 = 0.401$; $\bar{x}_3 = 0.408$; $\bar{x}_4 = 0.209$; $\bar{x}_5 = 0.212$; $\bar{x}_6 = 0.353$	$\sigma_1 = 30.984$ (K); $\sigma_2 = 0.241$; $\sigma_3 = 0.254$; $\sigma_4 = 2.79 \times 10^{-16}$; $\sigma_5 = 1.95 \times 10^{-16}$; $\sigma_6 = 8.92 \times 10^{-16}$	$\bar{y}_1 = 0.476$	$\sigma_{y_1} = 0.248$
II			$\bar{y}_2 = 0.491$	$\sigma_{y_2} = 0.250$

5. RESULT AND DISCUSSION

5.1 MLPNN-based Vapor-Liquid Equilibrium Modeling

RapidMiner studio [33] software were used to develop MLPNN-based models. It has a number of operators, including '*normalize*' for preprocessing input-output data and '*retrieve'* for retrieving stored input-output data from the repository and loading them into the process panel. The next operator is *'feed-forward neural net,'* which is trained by using an error-back propagation algorithm; *'apply model*,' which applies a model to a given set of examples; and '*performance* (*regression*),' which is used to assess statistical measures like *root mean squared error* (RMSE) and *correlation coefficient* (CC). The statistical measures RMSE and CC are used to analyze the prediction accuracy and generalization performance of MLPNN-based models. The values of RMSE and CC were evaluated for both training and test set data by using experimental and corresponding MLPNN-based model predicted values of dependent variables (outputs). The MLPNN-based optimal model was selected based on high CC and lower RMSE magnitudes for both training and test data sets.

The objective of this present study is to develop two MLPNN-based model I and II, for the prediction of the mole fraction of benzene (y_1) and cyclohexane (y_2) in vapor phase, respectively. A total of 117 isobaric VLE experimental data patterns of the ternary mixture (benzene-cyclohexane-anisole) reported in the literature [18] have been used in this study. This data consisting of the experimental conditions (temperature, and liquid and vapor phase compositions) and physiochemical properties (acentric factor) are given in Tables 2 and 4, respectively. The experimental data set of 117 input-output patterns has been randomly divided in a 3:1 ratio into the training (88 patterns) and the test (29 patterns) sets for the purpose of creating and analyzing the generalization ability of these model [34]. Although the former set was used to train MLPNN-based models across the entire range of experimental conditions, the latter was used to test their generalization ability.

Table-4: Physical properties of pure components involved in the study

Component	Acentric Factor (ω)
Benzene	$\omega_1 = 0.209$
Cyclohexane	$\omega_2 = 0.212$
Anisole	$\omega_3 = 0.353$

5.2 MLPNN-based Model-I for Prediction of Mole Fraction of Benzene in Vapor Phase (y_1)

The MLPNN-based model-I contains six inputs nodes (N=6), namely, mole fraction of benzene (x_1), and cyclohexane (x_2) in liquid phase, temperature (T), and acentric factors of benzene (ω_1), cyclohexane (ω_2), and anisole (ω_3). Single output node represent mole fraction of benzene (y_1) in vapor phase. The algorithm specific parameters, namely, learning rate (η), momentum (μ), number of hidden layers, and number of nodes in each hidden layer were all methodically speckled in order to obtain an optimal MLPNN model-I. MLPNN architectural and specific parameters have the following magnitudes: (i) hidden layer = 1, (ii) nodes in the hidden layer = 6, (iii) learning rate (η) = 0.5, and (iv) momentum (μ) = 0.05. Table 5 contains the design specifics of the optimal MLPNN-based model-I. Figure 2 depicts a schematic illustration of MLPNN-based model-I for predicting benzene vapor phase composition (y_1). For both the training and test data sets, the MLPNN models good prediction accuracy and generalization ability were assessed using CC and RMSE values; these magnitudes are given in Table 6. For the training and test data sets, the CC magnitudes with respect to y_1 predictions by the MLPNN-based model-I and the associated desired (experimental) values are 0.974 and 0.984, respectively, and the related RMSE magnitudes are 6.92 ×10-2 and 6.6 × 10-2, respectively. It can be observed that the MLPNN model–I has performed admirably in predicting and generalizing the mole fraction magnitudes of benzene in the vapor phase, based on the high (low) and comparable values of CC (RMSE) for both the training and test set data. The parity plot of the MLPNN-based model-I predicted values of the mole fraction of benzene in the vapor phase (y_1) and their experimental equivalents are shown in Fig. 3. The MLPNN-based model-I prediction accuracy and generalization ability are shown by the close agreement between model predicted y_1 and experimental values corresponding to both the training and test data sets.

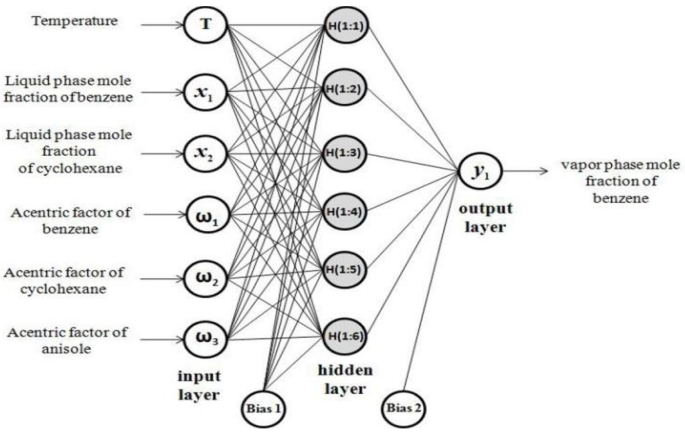

Fig-2: Schematic of MLPNN-based model-I for the prediction of vapor phase composition of benzene (y_1)

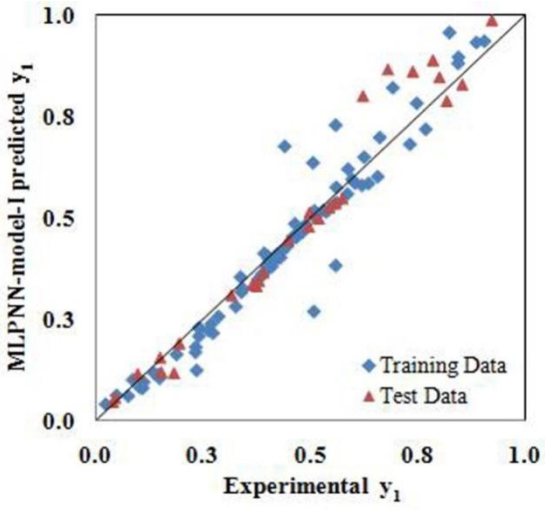

Fig-3: Parity plot of the experimental versus MLPNN-model-I predicted mole fractions of benzene in the vapor phase (y_1)

5.3 MLPNN-based Model-II for Prediction of Mole Fraction of Cyclohexane in Vapor Phase (y_2)

The MLPNN-based model-II predicting the mole fraction of cyclohexane in the vapor phase (y_2) was developed using same inputs as employed in the development of MLPNN-based model-I (see Tables 2 and 4). Overall, the best fit structural and training algorithm specific parameters such as (i) hidden layer = 1, (ii) nodes in hidden layer = 7, (iii) η = 0.5, and (iv) μ = 0.05 were used to develop MLPNN-based model-II. Table 5 shows the details of the optimal MLPNN-based model-II architecture. The MLPNN-based model-II prediction accuracy and generalization performance were assessed using CC and RMSE magnitudes for both training and test data sets, these are listed in Table 6. MLPNN-based model-II predictions reported high and comparable magnitudes of the coefficient of correlation (CC_{trn}=0.971; CC_{tst}=0.981), as well as low and comparable values of the root mean squared error ($RMSE_{trn}$ =7.32×10^{-2}; $RMSE_{tst}$ = 7.94× 10^{-2}) for both the training and test set data. A comparison of experimental values of a mole fraction of cyclohexane (y_2) in the vapor phase with predictions obtained by MLPNN-based model-II is shown in Fig. 4. As can be seen, for both training and test data, there is a good agreement between predicted values and their corresponding experimental values, demonstrating the MLPNN-based model-II has good prediction accuracy and generalization ability.

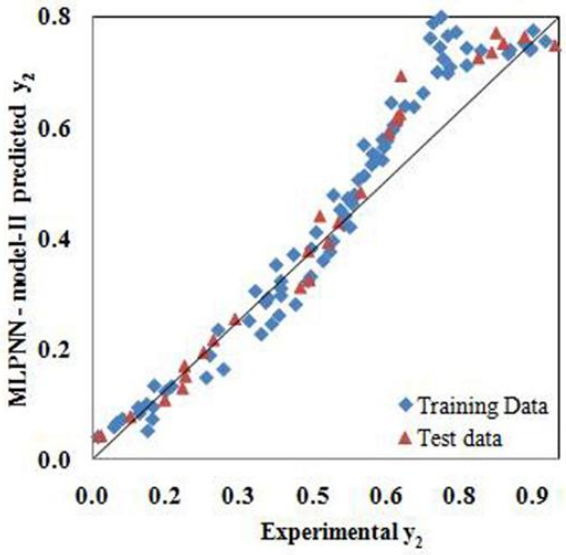

Fig-4: Parity plot of experimental versus MLPNN-model-II predicted mole fractions of cyclohexane in the vapor phase (y_2).

Table-6: Statistical analysis of MLPNN-based models for predicting vapor phase composition.

Model No.	Training set		Test set	
	CC_{trn}	$RMSE_{trn}$	CC_{tst}	$RMSE_{tst}$
I	0.974	6.92×10^{-2}	0.984	6.6×10^{-2}
II	0.971	7.32×10^{-2}	0.981	7.94×10^{-2}

6. CONCLUSION

The widely used feed-forward ANN, multi-layer perceptron (MLP), is being used in the study to develop MLPNN-based models for ternary system, benzene – cyclohexane -anisole, for predicting vapor-liquid equilibrium over a wide temperature range 351.03 - 421.09 K using experimental data collected from the literature. The input space in these models include temperature (T), mole fraction of benzene (x_1) and cyclohexane (x_2) in liquid phase, and acentric factors of benzene (ω_1), cyclohexane (ω_2) and anisole (ω_3). The output space contains mole fraction of benzene (y_1) and cyclohexane (y_2) in vapor-phase. An error-back propagation algorithm was utilized to train the models. The developed MLPNN-based models for the prediction of vapor phase composition have excellent output prediction accuracy and generalization ability as indicated by high CC and low RMSE magnitudes for both training and test data sets. The result shows good agreement between model predicted values and its corresponding experimental counterparts. So, artificial neural networks such as MLPNN can be a successful tool to represents complex nonlinear systems effectively as a prediction of VLE data, if developed efficiently. The MLPNN-based VLE modeling methodology described here can be used to develop similar models for a variety of different binary and ternary systems that are useful in industry.

ACKNOWLEDGEMENT

The authors gratefully acknowledge to Bharati Vidyapeeth (Deemed to be University) College of Engineering Pune-411043, India.

Table-5: Details of the architecture of the optimal MLPNN-based models and the corresponding EBP algorithm parameter value

Model No.	Output variable	Input nodes	Number of hidden layers	Number of hidden nodes	Transfer function for hidden nodes	Transfer function for output nodes	Momentum	Learning rate
I	y_1	6	1	6	Logistic sigmoid	Linear	0.5	0.05
II	y_2	6	1	7	Logistic sigmoid	Linear	0.5	0.05

REFERENCES

[1] A. Sporzynski, T. Hofman, A. Miskiewicz, A. Strutynska, L. Synoradzki, "Vapor-liquid equilibrium and density of the binary system 1-phenylethylamine + toluene," J. Chem. Eng. Data, vol. 50, 2005, pp. 33-35, doi:10.1021/je0499059.

[2] R. Wittig, J. Lohmann, J. Gmehling, "Vapor-liquid equilibria by UNIFAC group contribution 6. revision and extension," Ind. Eng. Chem. Res, vol. 42, 2003, pp. 183-188, doi: 10.1021/ie020506l.

[3] T. A. McFall, R. W. Hanks, J. J. Christensen, "The prediction of vapor-liquid equilibrium data from heat of mixing data for three non-ideal binary systems," Thermo. Acta vol. 60, 1983, pp. 327-339, doi:10.1016/0040-6031(83)80254-8.

[4] M.B. Mane, S.N. Shinde, "Vapor liquid equilibria: A review, Sci. Rev." Chem. Commun, vol. 2, 2012, pp. 158-171, https://www.tsijournals.com/articles/vapor-liquid-equilibria-a-review.pdf.

[5] B. Karunanithi, S. Shriniwasan, K. Bogeshwaran, "Modelling of vapour liquid equilibrium by artificial neural networks," Int. J. Comp. Eng. Res, vol. 4, 2014 pp.38-56, http://www.ijceronline.com/papers/Vol4_issue06/version-1/G04601038056.pdf.

[6] B. Vaferi, M. Lashkarbolooki, H. Esmaeili, A. Shariati. "Toward artificial intelligence-based modeling of vapor liquid equilibria of carbon dioxide and refrigerant binary systems," J. Serbian Chem. Soc, vol. 83, 2018, pp. 199-211, doi:10.2298/JSC170519088V.

[7] J. A. Freeman, D. M. Skapura, "Neural networks: algorithms, applications, and programming techniques," Addison- Wesley Longman Publishing Co., Inc., Reading, M. A., 1991. doi:10.1057/JORS.1992.170.

[8] M. Safamirzaei, H. Modarress, M. Mohsen-Nia, "Modeling the hydrogen solubility in methanol, ethanol, 1-propanol and 1-butanol," Fluid Phase Equili, vol. 289, 2010, pp. 32-39 doi:.10.1016/j.fluid.2009.10.012.

[9] C. Si-Moussa, S. Hanini, R. Derrichz, M. Bouhedda, A. Bouzidi, "Prediction of high-pressure vapor liquid equilibrium of six binary systems, carbon dioxide with six esters, using an artificial neural network model," Brazilian J. Chem. Eng, vol. 25, 2008, pp. 183-199 doi: 10.1590/S0104-66322008000100019.

[10] S. Atashrouz, H. Mirshekar, "Phase equilibrium modeling for binary systems containing CO_2 using artificial neural networks," Bulgarian Chem. Commun, vol. 46, 2014, pp. 104-116, http://www.bcc.bas.bg/bcc_volumes/Volume_46_Number_1_2014/15.pdf.

[11] B. Vaferi, Y. Rahnama, P. Darvishi, A. Toorani, M. Lashkarbolooki, "Phase equilibria modeling of binary systems containing ethanol using optimal feed-forward neural network," J. Supercrit. Fluids, vol. 84, 2013, pp. 80-88, doi:10.1016/j.supflu.2013.09.013.

[12] S. Ganguly, "Prediction of VLE data using radial basis function network," Comput. Chem. Eng, vol. 27, 2003, pp. 1445-1454, doi:10.1016/S0098-1354(03)00068-1.

[13] A. R. Moghadassi, M. R. Nikkholgh, S. M. Hosseini, F. Parvizian, A. Sanaeirad, "Vapour liquid equilibrium data prediction for binary systems containing propane," ARPN J. Eng. App. Sci, vol. 6, 2011, pp. 94-103,

[14] M. Dixit, J. Daniel, S. P. Bhattacharyya, "Exploring artificial neural networks to model interatomic and intermolecular potential energy surfaces," J of the Indian Chemical Soc, vol. 98, 2021, pp. 100114, doi:10.1016/j.jics.2021.100114.

[15] P. Goel, K. Saurabh, V. Patil-Shinde, S. S. Tambe, "Prediction of °API values of crude oils by use of saturates/aromatics/resins/asphaltenes analysis: computational-intelligence based model," SPE journal, vol. 22, 2017, pp. 817-853, doi: https://doi.org/10.2118/184391-PA

[16] V. Patil-Shinde, T. Kulkarni, R. Kulkarni, P. D. Chavan, T. Sharma, B. K. Sharma, S.S. Tambe, B. D. Kulkarni, "Artificial intelligence-based modeling of high ash coal gasification in a pilot plant scale fluidized bed gasifier," Ind. Eng. Chem. Res, vol. 53, 2014, pp. 18678–18689, doi:10.1021/ie500593j

[17] V. Patil-Shinde, S. Saha, B. K. Sharma, S. S. Tambe, B. D. Kulkarni, "High ash char gasification in thermo-gravimetric analyzer and prediction of gasification performance parameters using computational intelligence formalisms," Chem. Eng. Commun, vol. 203, 2016, pp. 1029–1044, doi:10.1080/00986445.2015.1135795

[18] B. Orge, G. Marino, M. Iglesias, L. M. Casas, J. Tojoa, "(Vapour + liquid) equilibria for the ternary system (benzene + cyclohexane + anisole) at P = 101.32 kPa," J. Chem. Thermo, vol. 33, 2001, pp. 1765–1776, doi:10.1006/jcht.2001.0882.

[19] G. M. Kontogeorgis, I. G. Economou, "Equations of state: from the ideas of van der Waals to association theories," J. Supercri. Fluids, vol. 55, 2010, pp. 421–437, doi:10.1016/j.supflu.2010.10.023.

[20] O. Redlich, J. N. Kwong, "On the thermodynamics of solutions. V. An equation of state. Fugacities of gaseous solutions," Chem. Rev, vol. 44, 1949, pp. 233-244, doi:10.1021/cr60137a013.

[21] G. Soave, "Equilibrium constants from a modified Redlich-Kwong equation of state," Chem. Eng. Sci, vol. 27, 1972, pp. 1197-1203, doi:10.1016/0009-2509(72)80096-4.

[22] D. Y. Peng, D. B. Robinson, "A new two-constant equation of state," Ind. Eng. Chem. Fundam, vol. 15, 1976, pp. 59-64, doi:10.1021/i160057a011.

[23] S. Ramdharee, E. Muzenda, M. Belaid, "A review of the equations of state and their applicability in phase equilibrium modeling," In International Conference on Chemical and Environmental Engineering, 2013, pp. 84-87.

[24] A. Correa, J. Tojo, J. M. Correa, A. Blanco, "New analytical solution of groups method parameters for the prediction of vapor-liquid equilibrium," Ind. Eng. Chem. Res, vol. 28, 1989, pp. 609-611, doi:10.1021/ie00089a017

[25] J. M. Smith, H. C. Van Ness, M. M. Abbott, "Introduction to Chemical Engineering Thermodynamics," McGraw-Hill, NY, 2005

[26] K. V. Narayana, "A Textbook of Chemical Engineering Thermodynamics," Prentice Hall of India Pvt. Ltd. 2013

[27] V. Vapnik. "The Nature of Statistical Learning Theory," Springer-Verlag, New York, 1995, doi:10.1007/978-1-4757-2440-0.

[28] J. Koza, "Genetic Programming: On the Programming of Computers by Means of Natural Selection," MIT Press, Cambridge, M.A, 1992.

[29] S. S. Tambe, P. B. Deshpande, B. D. Kulkarni, "Elements of Artificial Neural Networks with Selected Applications in Chemical Engineering, and Chemical & Biological Sciences," Simulation & Advanced Controls, Inc., Louisville, 1996.

[30] C. M. Bishop, "Neural networks and their applications," Rev. Sci. Instrum, vol. 65, 1994, pp. 1803-1832, doi:10.1063/1.1144830

[31] J. M. Zurada, "Introduction to Artificial Neural Systems, " Vol. 8, West Publ. Co., St. Paul, 1992.

[32] D. Rumelhart, G. Hinton, R. Williams, "Learning representations by back propagating error," Nature, vol. 323, 1986, pp. 533–536, doi:10.1038/323533a0.

[33] RapidMiner, RapidMiner studio 8.1: Visual Workflow for Predictive Analytics, https://rapidminer.com/products/studio, 2018, https://rapidminer.com/products/studio

[34] V. Patil-Shinde, S. S. Tambe, "Genetic programming based models for prediction of vapor-liquid equilibrium," Calphad, vol. 60, 2018, pp. 68–80. doi:10.1016/j.calphad.2017.11.002

[35] R. H. Perry, D. W. Green, "Perry's Chemical Engineers' Handbook," 8th ed., McGraw-Hill, NewYork, 2007.